

# Synthesis and Characterization of Pyridine Amide Cation Radical Complexes of Iron: Stabilization Due to Coordination with Low-Spin Iron(III) Center<sup>†</sup>

Apurba Kumar Patra, Manabendra Ray, and Rabindranath Mukherjee\*<sup>‡</sup>

Department of Chemistry, Indian Institute of Technology, Kanpur 208 016, India

Received August 12, 1999

We reported the synthesis and characterization of peptide complexes of low-spin iron(III) [Fe(bpb)(py)<sub>2</sub>][ClO<sub>4</sub>] (1) and Na[Fe(bpb)(CN)<sub>2</sub>] (2) [H<sub>2</sub>bpb = 1,2-bis(pyridine-2-carboxamido)benzene; py = pyridine], where iron is coordinated to four nitrogen donors in the equatorial plane with two amide nitrogen anions and two pyridine nitrogen donors (Ray, M.; Mukherjee, R.; Richardson, J. F.; Buchanan, R. M. *J. Chem. Soc., Dalton Trans.* **1993**, 2451). Chemical oxidation of 2 and a new low-spin iron(III) complex Na[Fe(Me<sub>6</sub>bpb)(CN)<sub>2</sub>]·H<sub>2</sub>O (4) [synthesized from a new iron(III) complex [Fe(Me<sub>6</sub>bpb)(py)<sub>2</sub>][ClO<sub>4</sub>] (3) (*S* = 1/2)] [H<sub>2</sub>Me<sub>6</sub>bpb = 1,2-bis(3,5-dimethylpyridine-2-carboxamido)-4,5-dimethylbenzene] by (NH<sub>4</sub>)<sub>2</sub>Ce(NO<sub>3</sub>)<sub>6</sub> afforded isolation of two novel complexes [Fe(bpb)(CN)<sub>2</sub>] (5) and [Fe(Me<sub>6</sub>bpb)(CN)<sub>2</sub>]·H<sub>2</sub>O (6). All the complexes have been characterized by physicochemical techniques. While 1–4 are brown/green, 5 and 6 are violet/bluish violet. The collective evidence from infrared, electronic, Mössbauer, and <sup>1</sup>H NMR spectroscopies, from temperature-dependent magnetic susceptibility data, and from cyclic voltammetric studies provides unambiguous evidence that 5 and 6 are low-spin iron(III) ligand cation radical complexes rather than iron(IV) complexes. Cyclic voltammetric studies on isolated oxidized complexes 5 and 6 display identical behavior (a metal-centered reduction and a ligand-centered oxidation) to that observed for complexes 2 and 4, respectively. The Mössbauer data for 6 are almost identical with those of the parent compound 4, providing compelling evidence that oxidation has occurred at the ligand in a site remote from the iron atom. Strong antiferromagnetic coupling ( $| -2J | \geq 450 \text{ cm}^{-1}$ ) of the *S* = 1/2 iron atom with the *S* = 1/2 ligand  $\pi$ -cation radical leads to an effectively *S* = 0 ground state of 5 and 6. The oxidized complexes display <sup>1</sup>H NMR spectra (in CDCl<sub>3</sub> solution), characteristic of diamagnetic species.

## Introduction

There has been a growing interest in the coordination chemistry of peptide complexes of iron in a +3 or higher oxidation state.<sup>1–8</sup> We<sup>1,2</sup> and others<sup>3–8</sup> have provided examples of structurally characterized complexes with coordinated carboxamido nitrogens as a part of macrocyclic as well as nonmacrocyclic ligand framework. It has been demonstrated that

transition metal complexes of dianionic bis(amide) ligands, derived from picolinic acid and 2,6-pyridinedicarboxylic acid, are subject to electrochemical oxidation at both the metal and the ligand to form metal- and ligand-centered oxidation products, respectively.<sup>1a,2,6,9,10</sup> Six-coordinate low-spin iron(III) complexes Na[Fe(bpb)(CN)<sub>2</sub>]<sup>1a</sup> and [Fe(bpc)(L)<sub>2</sub>][ClO<sub>4</sub>]<sup>6</sup> [H<sub>2</sub>bpc = 1,2-bis(pyridine-2-carboxamido)-4,5-dichlorobenzene; L = Bu<sub>3</sub>P, Im, 1-MeIm, <sup>t</sup>Bu(py)] are reported to exhibit well-behaved one-electron oxidation processes, but the products have not been isolated, and their full characterization was never attempted. Our approach to this problem has been to work out a synthetic method that would allow the oxidized species to be isolated in the analytically pure form and to assign the correct formulation of these species. Here we report the isolation and characterization of two new low-spin iron(III) complexes [Fe(Me<sub>6</sub>bpb)(py)<sub>2</sub>][ClO<sub>4</sub>] and Na[Fe(Me<sub>6</sub>bpb)(CN)<sub>2</sub>]·H<sub>2</sub>O [H<sub>2</sub>Me<sub>6</sub>bpb = 1,2-bis(3,5-dimethylpyridine-2-carboxamido)-4,5-dimethylbenzene; py = pyridine] and one-electron oxidized products of Na[Fe(bpb)(CN)<sub>2</sub>]<sup>1a</sup> and Na[Fe(Me<sub>6</sub>bpb)(CN)<sub>2</sub>]·H<sub>2</sub>O. We find that oxidized complexes [Fe(bpb)(CN)<sub>2</sub>] and [Fe(Me<sub>6</sub>bpb)(CN)<sub>2</sub>]·H<sub>2</sub>O are diamagnetic due to antiferromagnetic coupling between the unpaired electron of the low-spin iron(III) state and the unpaired electron of the ligand  $\pi$ -cation radical, as revealed

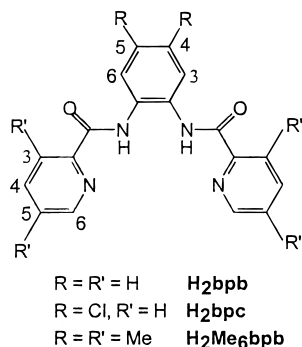
<sup>†</sup> Dedicated to Professor Animesh Chakravorty on the occasion of his 65th birthday.

<sup>‡</sup> E-mail: rnm@iitk.ac.in.

- (1) (a) Ray, M.; Mukherjee, R.; Richardson, J. F.; Buchanan, R. M. *J. Chem. Soc., Dalton Trans.* **1993**, 2451 and references therein. (b) Patra, A. K.; Mukherjee, R. *Polyhedron* **1999**, *18*, 1317.
- (2) Ray, M.; Ghosh, D.; Shirin, Z.; Mukherjee, R. *Inorg. Chem.* **1997**, *36*, 3568.
- (3) (a) Noveron, J. C.; Olmstead, M. M.; Mascharak, P. K. *Inorg. Chem.* **1998**, *37*, 1138. (b) Marlin, D. S.; Olmstead, M. M.; Mascharak, P. K. *Inorg. Chem.* **1999**, *38*, 3258.
- (4) (a) Tao, X.; Stephan, D. W.; Mascharak, P. K. *Inorg. Chem.* **1987**, *26*, 754. (b) Brown, S. J.; Olmstead, M. M.; Mascharak, P. K. *Inorg. Chem.* **1990**, *29*, 3229.
- (5) Yang, Y.; Diederich, F.; Valentine, J. S. *J. Am. Chem. Soc.* **1991**, *113*, 7195.
- (6) Che, C.-M.; Leung, W.-H.; Li, C.-K.; Cheng, H.-Y.; Peng, S.-M. *Inorg. Chim. Acta* **1992**, *196*, 43.
- (7) Wocadlo, S.; Massa, W.; Folgado, J.-V. *Inorg. Chim. Acta* **1993**, *207*, 199.
- (8) (a) Collins, T. J.; Kostka, K. L.; Münck, E.; Uffelman, E. S. *J. Am. Chem. Soc.* **1990**, *112*, 5637. (b) Collins, T. J.; Fox, B. G.; Hu, Z. G.; Kostka, K. L.; Münck, E.; Rickard, C. E. F.; Wright, L. J. *J. Am. Chem. Soc.* **1992**, *114*, 8724. (c) Kostka, K. L.; Fox, B. G.; Hendrich, M. P.; Collins, T. J.; Rickard, C. E. F.; Wright, L. J.; Münck, E. J. *J. Am. Chem. Soc.* **1993**, *115*, 6746. (d) Bartos, M. J.; Kidwell, C.; Kauffmann, K. E.; Gordon-Wylie, S. W.; Collins, T. J.; Clark, G. C.; Münck, E.; Weintraub, S. T. *Angew. Chem., Int. Ed. Engl.* **1995**, *34*, 1216.

- (9) (a) Ray, M.; Mukherjee, S.; Mukherjee, R. *J. Chem. Soc., Dalton Trans.* **1990**, 3635. (b) Ray, M.; Mukherjee, R. *Polyhedron* **1992**, *11*, 2625. (c) Patra, A. K.; Mukherjee, R. *Inorg. Chem.* **1999**, *38*, 1388.
- (10) (a) Mak, S.-T.; Yam, V. W.-W.; Che, C.-M.; Mak, T. C. W. *J. Chem. Soc., Dalton Trans.* **1990**, 2555. (b) Leung, W.-H.; Ma, J.-X.; Yam, V. W.-W.; Che, C.-M.; Poon, C.-K. *J. Chem. Soc., Dalton Trans.* **1991**, 1071. (c) Mak, S.-T.; Wong, W.-T.; Yam, V. W.-W.; Lai, T.-F.; Che, C.-M. *J. Chem. Soc., Dalton Trans.* **1991**, 1915.

by solid-state, temperature-dependent magnetic susceptibility and room-temperature Mössbauer spectral measurements. In addition to this evidence, diamagnetic ground state of  $[\text{Fe}(\text{bpb})(\text{CN})_2]$  and  $[\text{Fe}(\text{Me}_6\text{bpb})(\text{CN})_2]\cdot\text{H}_2\text{O}$  has been confirmed from their  $^1\text{H}$  NMR spectra.



## Experimental Section

**Materials and Reagents.** Commercial reagents were used as obtained without further purification. Solvents were dried as reported previously.<sup>12</sup> 3,5-Dimethylpyridine-2-carboxylic acid was prepared following literature reports.<sup>11</sup>  $[\text{Fe}(\text{MeCN})_4][\text{ClO}_4]_2$  and tetra-*n*-butylammonium perchlorate (TBAP) were prepared/purified as before.<sup>1a,2</sup>

**Syntheses.** **1,2-Bis(Pyridine-2-carboxamido)Benzene (H<sub>2</sub>bpb).** This was prepared as reported previously.<sup>12</sup>

**1,2-Bis(3,5-Dimethylpyridine-2-carboxamido)-4,5-Dimethylbenzene (H<sub>2</sub>Me<sub>6</sub>bpb).** To a stirred solution of 3,5-dimethylpyridine-2-carboxylic acid (0.5 g, 0.003 mol) in pyridine (2 mL), a solution of 4,5-dimethyl-1,2-diaminobenzene (0.225 g, 0.0016 mol) in pyridine (1 mL) was added dropwise. The solution was stirred for 15 min and triphenyl phosphite (1.026 g, 0.003 mol) was added dropwise. The temperature of the reaction mixture was warmed at 100 °C, and the mixture was magnetically stirred for 4 h. The volume was then reduced to ~2 mL and kept in air. After 24 h, a white precipitate that resulted was collected by filtration. Recrystallization from  $\text{CHCl}_3/n$ -hexane afforded white needles. Yield: 0.37 g (55%).  $^1\text{H}$  NMR ( $\text{CDCl}_3$ ):  $\delta$  10.29 (2 H, s, NH), 8.23 (2 H, s, py 6-H), 7.68 [2 H, s, benzamide (bz) 3-H], 7.45 (2 H, s, py 4-H), 2.87 (6 H, s, py 3-Me), 2.42 (6 H, s, bz 4,5-Me), 2.36 (6 H, s, py 5-Me).

**Synthesis of Metal Complexes.**  $[\text{Fe}(\text{bpb})(\text{py})_2][\text{ClO}_4]$  (**1**) and  $\text{Na}[\text{Fe}(\text{bpb})(\text{CN})_2]$  (**2**) were synthesized as described previously.<sup>1a</sup>

**CAUTION!** Transition metal perchlorates are hazardous and may explode. Only small quantities should be prepared, and they should be used with great care.

**$[\text{Fe}(\text{Me}_6\text{bpb})(\text{py})_2][\text{ClO}_4]$  (**3**).** A solution of  $[\text{Fe}(\text{MeCN})_4][\text{ClO}_4]_2$  (0.104 g, 0.248 mmol) in MeCN (5 mL) was added slowly to a magnetically stirred solution containing the ligand H<sub>2</sub>Me<sub>6</sub>bpb (0.1 g, 0.248 mmol) and pyridine (0.08 g, 0.995 mmol) in MeCN (10 mL). After 2 h, the resulting solution was cooled in a refrigerator. The reddish-brown crystalline precipitate that formed was collected by filtration and washed with ~1 mL of cold MeCN, and dried in vacuo (yield: 0.16 g, ~92%).

**Characterization.** Anal. Calcd for  $\text{C}_{34}\text{H}_{34}\text{N}_6\text{O}_6\text{ClFe}$ : C, 57.40; H, 4.52; N, 11.44. Found: C, 57.18; H, 4.76; N, 11.77. IR (KBr,  $\text{cm}^{-1}$ , selected peaks): 1620  $\nu(\text{CO})$ , 1100, and 620 ( $\nu(\text{ClO}_4)$ ). Conductivity (~1 mM solution in pyridine at 298 K):  $\Lambda_M = 34 \Omega^{-1} \text{cm}^2 \text{mol}^{-1}$  (corresponding value for TBAP:  $30 \Omega^{-1} \text{cm}^2 \text{mol}^{-1}$ ). Absorption spectrum [ $\lambda_{\text{max}}$ , nm ( $\epsilon$ ,  $\text{M}^{-1} \text{cm}^{-1}$ )] (in pyridine): 400 sh (3600), 548 (1100), 930 (1030).

**$\text{Na}[\text{Fe}(\text{Me}_6\text{bpb})(\text{CN})_2]\cdot\text{H}_2\text{O}$  (**4**).** To a reddish-brown suspension of  $[\text{Fe}(\text{Me}_6\text{bpb})(\text{py})_2][\text{ClO}_4]$  (**3**) (0.32 g, 0.448 mmol) in ethanol (20 mL)

was added solid NaCN (0.25 g, 5.082 mmol) and the mixture was allowed to stir for 2 h. A deep-green solution thus generated was completely removed in vacuo. DMF (10 mL) was added to the residue and filtered to remove excess NaCN. The solvent was then removed under reduced pressure, and ethanol (8 mL) was added to the residue. After addition of diethyl ether (10 mL), the mixture was kept in a refrigerator for 12 h. The crystalline compound that precipitated out was collected by filtration and dried in vacuo (yield: 0.13 g, ~88%).

**Characterization.** Anal. Calcd for  $\text{C}_{26}\text{H}_{26}\text{N}_6\text{O}_3\text{NaFe}$ : C, 56.83; H, 4.73; N, 15.30. Found: C, 56.15; H, 4.80; N, 15.53. IR (KBr,  $\text{cm}^{-1}$ , selected peaks): 3450 ( $\nu(\text{OH})$ ), 2120 ( $\nu(\text{CN})$ ), 1600 ( $\nu(\text{CO})$ ). Conductivity (MeCN, ~1 mM solution at 298 K):  $\Lambda_M = 115 \Omega^{-1} \text{cm}^2 \text{mol}^{-1}$ . Absorption spectrum [ $\lambda_{\text{max}}$ , nm ( $\epsilon$ ,  $\text{M}^{-1} \text{cm}^{-1}$ )] (in MeCN): 240 sh (19 450), 273 (14 950), 298 sh (9730), 370 (8460), 430 sh (6 150), 580 sh (960), 760 (1500).

**$[\text{Fe}(\text{bpb})(\text{CN})_2]$  (**5**).** To a magnetically stirred solution of  $\text{Na}[\text{Fe}(\text{bpb})(\text{CN})_2]$  (**2**) (0.1 g, 0.224 mmol) in MeCN (10 mL), a solution of  $(\text{NH}_4)_2\text{Ce}(\text{NO}_3)_6$  (0.16 g, 0.292 mmol) in MeCN (5 mL) was added dropwise. Dark-violet compound that precipitated out was collected by filtration and washed with MeCN until the washings became colorless. The solid thus obtained was dried in vacuo (yield: 0.08 g, ~84%).

**Characterization.** Anal. Calcd for  $\text{C}_{20}\text{H}_{12}\text{N}_6\text{O}_2\text{Fe}$ : C, 56.63; H, 2.85; N, 19.81. Found: C, 56.28; H, 2.95; N, 19.72. IR (KBr,  $\text{cm}^{-1}$ , selected peaks): 2120 ( $\nu(\text{CN})$ ), 1670 ( $\nu(\text{CO})$ ). Conductivity (DMF, ~1 mM solution at 298 K):  $\Lambda_M = 5 \Omega^{-1} \text{cm}^2 \text{mol}^{-1}$ . Absorption spectrum [in DMF;  $\lambda_{\text{max}}$ , nm ( $\epsilon$ ,  $\text{M}^{-1} \text{cm}^{-1}$ )]: 290 (7100), 358 (6620), 410 sh (5020), 545 (2650), 699 (1200)].  $^1\text{H}$  NMR (200 MHz,  $\text{CDCl}_3$ ; very dilute solution):  $\delta$  9.38 (2 H, d, py 6-H), 8.77 (2 H, d, bz 3/6-H), 8.29 (4 H, m, bz 4/5-H), 7.77 (4 H, m, py 4/5-H).

**$[\text{Fe}(\text{Me}_6\text{bpb})(\text{CN})_2]\cdot\text{H}_2\text{O}$  (**6**).** Ceric ammonium nitrate (0.065 g, 0.113 mmol) dissolved in MeCN (2 mL) was added dropwise to a vigorously magnetically stirred solution (MeCN–H<sub>2</sub>O: 3 mL/0.5 mL) of  $\text{Na}[\text{Fe}(\text{Me}_6\text{bpb})(\text{CN})_2]\cdot\text{H}_2\text{O}$  (**4**) (0.05 g, 0.094 mmol). The resulting bluish-violet solution was stirred for a further 2 h. The violet compound that precipitated out was collected by filtration and washed with cold MeCN (~1 mL). Recrystallization from  $\text{CHCl}_3/n$ -hexane afforded pure compound as a bluish-violet solid, which was air-dried (yield: 0.035 g, ~73%).

**Characterization.** Anal. Calcd for  $\text{C}_{26}\text{H}_{26}\text{N}_6\text{O}_3\text{Fe}$ : C, 59.31; H, 4.94; N, 15.97. Found: C, 59.67; H, 4.85; N, 15.86. IR (KBr,  $\text{cm}^{-1}$ , selected peaks): 3450 ( $\nu(\text{OH})$ ), 2120 ( $\nu(\text{CN})$ ), 1670 ( $\nu(\text{CO})$ ). Conductivity (DMF, ~1 mM solution at 298 K):  $\Lambda_M = 7 \Omega^{-1} \text{cm}^2 \text{mol}^{-1}$ . Absorption spectrum [ $\lambda_{\text{max}}$ , nm ( $\epsilon$ ,  $\text{M}^{-1} \text{cm}^{-1}$ )]: ( $\text{CH}_2\text{Cl}_2$ ) 240 sh (23 850), 266 (21 300), 310 (12 800), 355 (10 100), 392 (9300), 450 sh (4400), 563 (8850), 695 sh (1950), 775 sh (1270).  $^1\text{H}$  NMR (400 MHz,  $\text{CDCl}_3$ ):  $\delta$  9.09 (2 H, s, py 6-H), 7.77 (2 H, s, 3/6-H), 7.47 (2 H, s, py 4-H), 2.98 (6 H, s, py 3-Me), 2.36 (6 H, s, bz 4,5-Me), 1.67 (2 H, s, H<sub>2</sub>O), 1.40 (6 H, s, py 5-Me).

**Physical Measurements.** Elemental analyses were obtained from the Department of Inorganic Chemistry, Indian Association for the Cultivation of Science, Calcutta, India. Conductivity measurements were done with an Elico type CM-82T conductivity bridge (Hyderabad, India) with solute concentrations of ~1 mM. Spectroscopic measurements were made using the following instruments: IR (KBr, 4000–600  $\text{cm}^{-1}$ ), Perkin-Elmer M-1320; electronic, Perkin-Elmer Lambda 2; X-band EPR, Varian 109 C (fitted with a quartz dewar for measurements at liquid–dinitrogen temperature). The spectra were calibrated with diphenylpicrylhydrazyl, DPPH ( $g = 2.0037$ ).  $^1\text{H}$  NMR spectra were recorded using either a Bruker WP-80 (80 MHz) or a JEOL-JNM-LA 400 FT (400 MHz) spectrometer. For complex **5** the spectrum was recorded on a Bruker AC(AF)-200 MHz spectrometer at the Indian Institute of Science, Bangalore, India. Mössbauer measurements at 300 K were made on a standard, constant-acceleration spectrometer (Department of Physics). Isomer shift values ( $\delta$ ) are given with respect to metallic iron at 300 K.

**Magnetic Measurements.** Solid-state magnetic data were collected in the 25–300 K range (for **6** in the 63–300 K range) with a locally built Faraday device equipped with an electromagnet with constant gradient pole caps (Polytronic Corporation, Mumbai, India), Sartorius M25-D/S balance (Göttingen, Germany), a closed-cycle refrigerator,

(11) (a) Augustinsson, K.-B.; Hasselquist, H. *Acta Chem. Scand.* **1961**, *15*, 817. (b) Takahashi, K.; Takeda, K.; Mitsuhashi, K. *J. Heterocycl. Chem.* **1978**, *15*, 893.

(12) Barnes, D. J.; Chapman, R. L.; Vagg, R. S.; Watton, E. C. *J. Chem. Eng. Data* **1978**, *23*, 349.

and a Lake Shore temperature controller (Cryo Industries, USA). All measurements were made at a fixed main field strength of  $\sim 10$  kG. The calibration of the system and details of measurements are already reported in the literature.<sup>1b,2</sup> The temperature dependence of the molar susceptibility of **5** and **6** were analyzed by using the van Vleck equation with the eigenvalues of the spin coupling Hamiltonian ( $H = -2JS_1S_2$ ,  $S_1 = S_2 = 1/2$ ). This gives rise to eq 1:<sup>13</sup>

$$\chi_M = N\beta^2 g^2 / kT [2 \exp(2J/kT) / 1 + 3 \exp(2J/kT)] \quad (1)$$

where  $\chi_M$  is the molar susceptibility and other symbols have their usual meanings. The fit of the data to the van Vleck equation was improved by the addition of a small amount of low-spin Fe(III) impurity and a temperature-independent-paramagnetism (TIP) term. Thus eq 1 was modified in the following manner:

$$\chi_M = (1 - P)\chi' + P\chi_c + \text{TIP} \quad (2)$$

where  $\chi_M$  is the total calculated susceptibility,  $\chi'$  is the spin-coupled susceptibility calculated from eq 1,  $\chi_c$  is the assumed Curie law magnetic susceptibility for the low-spin Fe(III) impurity [ $= N\beta^2 g^2 S(S+1)/3kT$ ], and  $P$  is the fraction of the paramagnetic impurity.

Solution-state magnetic susceptibilities were obtained by the NMR technique of Evans<sup>14</sup> in pyridine or in MeCN with a PMX-60 JEOL (60 MHz) NMR spectrometer. Susceptibilities (in  $\text{cm}^3 \text{mol}^{-1}$ ) were corrected<sup>13</sup> for diamagnetic contributions.

**Electrochemical Measurements.** Cyclic voltammetric experiments were performed by using a PAR model 370 electrochemistry system consisting of a M-174A polarographic analyzer, a M-175 universal programmer, and an RE 0074 X-Y recorder. The cell contained a glassy carbon working electrode (PAR model G0021), a Pt wire auxiliary electrode, and a saturated calomel electrode (SCE) as reference electrode. The measured redox potentials at 298 K were converted to the ferrocenium/ferrocene ( $\text{Fc}^+/\text{Fc}$ ) reference.<sup>15</sup> Details of the cell configuration are as described before.<sup>1a,2,9a</sup>

## Results and Discussion

**Synthesis.** The new pyridine amide ligand  $\text{H}_2\text{Me}_6\text{bpb}$  was designed to increase the solubility of the resulting complexes in organic solvents for a better evaluation of their solution-state properties, compared to its congener  $\text{H}_2\text{bpb}$ . Moreover, because of the presence of six methyl groups on the ligand periphery, it is expected that  $\text{Me}_6\text{bpb}(2-)$  would act as a better  $\sigma$ -donor toward metal ions. It was prepared by treating 3,5-dimethylpyridine-2-carboxylic acid (synthesized from 3,5-dimethylaniline, following reported organic synthetic methodologies)<sup>11</sup> with 4,5-dimethyl-1,2-phenylenediamine in the presence of triphenyl phosphite in pyridine.<sup>12</sup> The synthesis of iron(III) cyanide complexes **2** and **4** involved initial synthesis of iron(III) pyridine complexes **1** and **3** from the reaction between the corresponding ligand, pyridine, and  $[\text{Fe}(\text{MeCN})_4][\text{ClO}_4]_2$ .

Clean one-electron chemical oxidation of **2** in MeCN (in which the complex is only partially soluble, giving rise to a green coloration) by 1.3 equiv of  $(\text{NH}_4)_2\text{Ce}(\text{NO}_3)_6$  initiated the precipitation of a violet-colored microcrystalline compound,  $[\text{Fe}(\text{bpb})(\text{CN})_2]$  **5**. However, clean oxidation of **4** in 1:6  $\text{H}_2\text{O}$ –MeCN solvent mixture (v/v) by 1.2 equiv of  $(\text{NH}_4)_2\text{Ce}(\text{NO}_3)_6$  generated a deep bluish-violet solution, which on usual workup led to the isolation of the oxidized product as a highly crystalline bluish-violet solid,  $[\text{Fe}(\text{Me}_6\text{bpb})(\text{CN})_2] \cdot \text{H}_2\text{O}$  **6**.

The absence of  $\nu(\text{N}-\text{H})$  in the IR spectra of these complexes indicates that the ligands are coordinated in the deprotonated

form. Interestingly, compared to the corresponding iron(III) complexes, the oxidation results in a pronounced increase in the C–O IR stretching frequencies of  $\nu(\text{amide I})$  vibration.<sup>16,17</sup> In fact, the shift is  $\sim 60 \text{ cm}^{-1}$  between **2** and **5**, and it is  $\sim 70 \text{ cm}^{-1}$  between **4** and **6** (Figures S1 and S2, Supporting Information). We believe this behavior is diagnostic of ligand oxidation (vide infra). A similar shift in the C–O IR stretching frequencies, between an anionic cobalt(III) complex and its one-electron oxidized counterpart, is reported for a macrocyclic amide system of Collins et al.<sup>18</sup> For **4–6**,  $\nu(\text{CN})$  occurs at  $2120 \text{ cm}^{-1}$ . Complexes **1–4** behave as 1:1 electrolyte.<sup>19</sup> As expected, the oxidized complexes **5** and **6** are nonconducting in DMF. Complex **6** is soluble in  $\text{CHCl}_3$ ,  $\text{CH}_2\text{Cl}_2$ , MeCN, DMF, and acetone. Its solubility even in nonpolar solvents such as  $\text{CHCl}_3$  and  $\text{CH}_2\text{Cl}_2$  justifies its neutral nature. Elemental analyses, IR, and solution electrical conductivity data are in good agreement with the above formulations. Unfortunately, we have not succeeded so far in growing single crystals of either of the oxidized complexes, suitable for X-ray diffraction studies.

**Cyclic Voltammetry. (a) Metal Reduction of Iron(III) Complexes.** The electrochemical behavior of **1–6** has been studied by cyclic voltammetry (CV) and the results are in Table 1. The one-electron nature of the redox response of **3** has been confirmed by comparison of current height with the response of samples of **1** or **2**,<sup>1a</sup> under the same experimental conditions. The wave is ascribed to the  $\text{Fe}^{\text{III}}-\text{Fe}^{\text{II}}$  couple. The  $E_{1/2}$  value is  $\sim 200 \text{ mV}$  more cathodic than that of **1**,<sup>1a</sup> indicating that the methyl-substituted tetradentate dinegative peptide ligand  $\text{Me}_6\text{bpb}(2-)$  strongly stabilizes the iron(III) state toward reduction. The corresponding couple for **2**<sup>1a</sup> and **4** follows a similar trend.

**(b) Ligand Oxidation of Iron(III) Complexes.** As observed for **2**,<sup>1a</sup> complex **4** in DMF solution exhibits an additional response (Table 1). Tetradentate pyridine amide ligands<sup>1,5,6,9a,b,10</sup> are derived from 1,2-diaminobenzene or its 4,5-disubstituted derivatives. It has been demonstrated that the 1,2-diaminobenzene ring is susceptible to oxidation, generating a cation radical.<sup>1a,6,9a,b,10,18</sup> Based on the reported redox properties of transition metal complexes of pyridine amide ligands, we assign that the  $\pi$  system in the 1,2-diaminobenzene ring is the expected site of oxidation (vide infra).

In DMF solution ( $\sim 1 \text{ mM}$ ), the oxidized iron complex of unsubstituted ligand  $[\text{Fe}(\text{bpb})(\text{CN})_2]$  **5** reverts back to iron(III) species  $[\text{Fe}(\text{bpb})(\text{CN})_2]^-$  within  $\sim 2 \text{ h}$ . We suspect that because of its high reduction potential the oxidized species **5** oxidizes trace water<sup>20</sup> present in the solvent. For this reason, we synthesized the complex  $\text{Na}[\text{Fe}(\text{Me}_6\text{bpb})(\text{CN})_2] \cdot \text{H}_2\text{O}$  **4** to tune the corresponding couple at a lower potential to enhance the stability of the desired oxidized complex in water (see Experimental Section).

**(c) Redox Processes of Isolated Oxidized Complexes.** CV studies on isolated oxidized complexes **5** and **6** display identical behavior to that observed for complexes **2** and **4**, respectively (Table 1). The cyclic behavior of  $[\text{Fe}(\text{Me}_6\text{bpb})(\text{CN})_2] \cdot \text{H}_2\text{O}$  **6** in  $\text{CH}_2\text{Cl}_2$  is displayed in Figure 1. This documents the purity and authenticity of the isolated oxidized complex.

**Absorption Spectra.** The absorption spectral studies are the easiest means of characterization of iron(III) complexes as well

(13) O'Connor, C. J. *Prog. Inorg. Chem.* **1992**, *32*, 233.

(14) Evans, D. F. *J. Chem. Soc.* **1959**, 2003.

(15) Under our experimental conditions, the  $E_{1/2}$  values (V) for couple  $\text{Fc}^+/\text{Fc}$  were 0.40 (MeCN), 0.49 (DMF), 0.49 ( $\text{CH}_2\text{Cl}_2$ ), and 0.52 (py) vs SCE.

(16) Chapman, R. L.; Vagg, R. S. *Inorg. Chim. Acta* **1979**, *33*, 227.

(17) Patra, A. K.; Ray, M.; Mukherjee, R. *J. Chem. Soc., Dalton Trans.* **1999**, 2461.

(18) Collins, T. J.; Powell, R. D.; Slebochnick, C.; Uffelman, E. S. *J. Am. Chem. Soc.* **1991**, *113*, 8419.

(19) Geary, W. J. *Coord. Chem. Rev.* **1971**, *7*, 81.

(20) Gupta, N.; Mukherjee, S.; Mahapatra, S.; Ray, M.; Mukherjee, R. *Inorg. Chem.* **1992**, *31*, 139.



**Table 1.** Magnetic, Mössbauer, EPR, and Cyclic Voltammetric Data of Iron Complexes

complex	$\mu_{\text{eff}}^{300\text{K}}$ ( $\mu_{\text{B}}$ )		Mössbauer (300 K)		EPR (77 K): <i>g</i>	CV: $E_{1/2}$ , V vs $\text{Fc}^+/\text{Fc}$ ( $\Delta E_p$ , mV)
	solid	solution	$\delta$ , mm/s	$\Delta E_Q$ , mm/s		
<b>1</b>	2.44 <sup>a</sup>	2.50 <sup>a,b</sup>	0.12	2.36	2.258, 2.182, 1.943 (solid) <sup>a</sup>	-0.58 (150) <sup>a,b</sup>
<b>2</b>	2.23	2.10 <sup>a,c</sup>	-0.04	1.35	2.13 (solid) <sup>a</sup>	-1.32 (100) <sup>a,c</sup> 0.17 (80) <sup>a,c</sup>
<b>3</b>	2.28	2.25 <sup>b</sup>			2.218, 1.955 (DMF) <sup>a</sup> 2.203, 1.952 (solid)	-0.77 (60) <sup>b</sup>
<b>4</b>	1.80	2.02 <sup>d</sup>	0.00	1.21	2.204, 1.959 (py) 2.260, 2.195, 2.133, 1.945 (solid)	-1.55 (80) <sup>c</sup> -0.09 (200) <sup>c</sup> -1.35 (100) <sup>d</sup> -0.03 (60) <sup>d</sup>
<b>5</b>	0.81		-0.08	1.62	2.138 <sup>d,e</sup>	<sup>g</sup>
<b>6</b>	1.18		0.00	1.24	<sup>f</sup>	-1.45 (120) <sup>h</sup> -0.15 (120) <sup>h</sup>

<sup>a</sup> Reference 1a. <sup>b</sup> In pyridine. <sup>c</sup> In DMF. <sup>d</sup> In MeCN. <sup>e</sup> At 300 K. <sup>f</sup> EPR silent. <sup>g</sup> Identical to that of **2**. <sup>h</sup> In  $\text{CH}_2\text{Cl}_2$ .

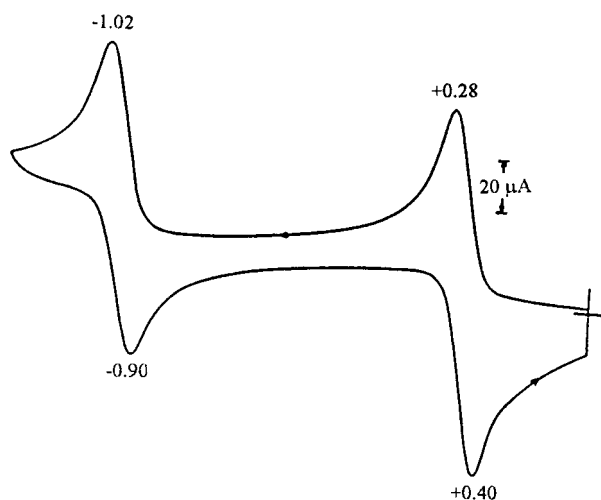


**Figure 1.** Cyclic voltammogram (50 mV/s) of a 0.95-mM solution of  $[\text{Fe}(\text{Me}_6\text{bpb})(\text{CN})_2]\cdot\text{H}_2\text{O}$  (**6**) at a glassy carbon electrode in dichloromethane (0.15 M in TBAP). Indicated potentials (in V) are vs SCE.

as their one-electron oxidized products. As was observed<sup>1a</sup> for **1** and **2**, in the visible region the absorption spectra of the new low-spin iron(III) complexes **3** and **4** are dominated by LMCT transitions. The oxidized compounds are clearly identifiable by their characteristic absorption feature, with enhancement in extinction coefficients compared to their iron(III) counterparts. A similar behavior was observed before.<sup>6</sup> The absorption spectra of **4** and **6** are displayed in Figure 2.

**EPR Spectra of Iron(III) Complexes.** The EPR spectra of low-spin iron(III) complexes **1** and **2** were analyzed to determine the ligand-field parameters.<sup>1a</sup> The ground state of both complexes was consistent with the electronic distribution  $(d_{xz,yz})^4(d_{xy})^1$ . The EPR spectral results at 77 K of **1–4** in the solid state as well as in solution are in Table 1. Complex **3** displays axial spectra. In the polycrystalline state (300 K), **4** exhibits an axial spectrum with *g* values of 2.172 and 1.953. At 77 K it displays an anisotropic spectrum (Figure S3, Supporting Information). In MeCN solution (300 K),<sup>21</sup> complex **4** shows only a broad isotropic signal.

**Magnetism and Mössbauer Spectra. (a) Iron(III) Complexes.** To confirm the spin state of the iron(III) centers in **2–4**, variable-temperature (25–300 K) magnetic susceptibility measurements were performed on powdered samples using the Faraday method. The  $\mu_{\text{eff}}$  values (300 K) of **1–4** (Table 1) and the temperature-dependent behavior of **2–4** (Figures S4–S6,

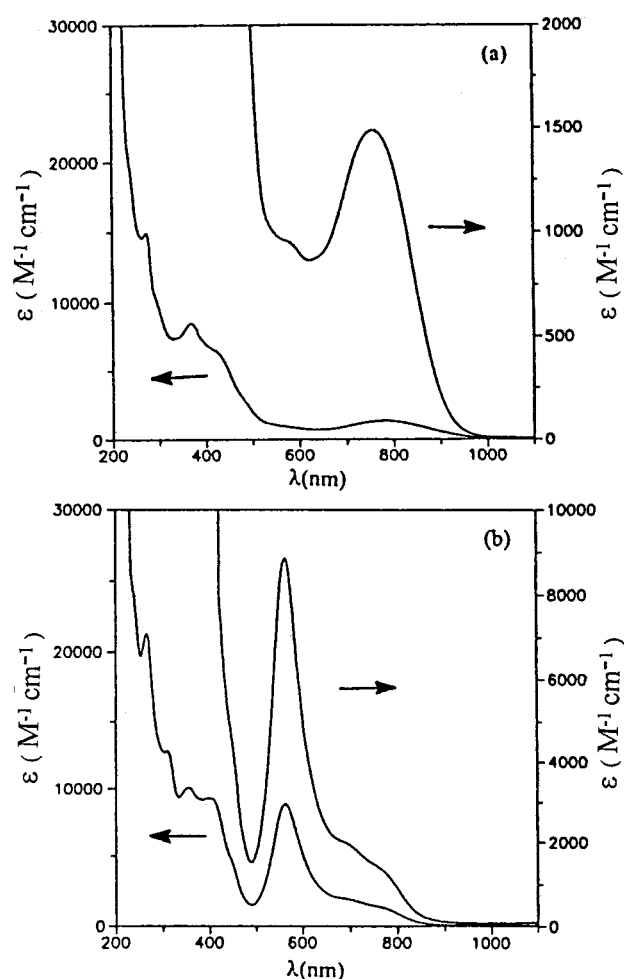


**Figure 2.** Electronic absorption spectra of (a)  $\text{Na}[\text{Fe}(\text{Me}_6\text{bpb})(\text{CN})_2]\cdot\text{H}_2\text{O}$  (**4**) (in MeCN) and (b)  $[\text{Fe}(\text{Me}_6\text{bpb})(\text{CN})_2]\cdot\text{H}_2\text{O}$  (**6**) (in dichloromethane).

Supporting Information) correspond to the  $S = 1/2$  state.<sup>1a,2</sup> Appreciable orbital contribution<sup>22</sup> was revealed in the case of **3**; however, it is much lower for complex **4**. A similar trend was observed between **1** and **2**.<sup>1a</sup> For **2–4**, as the temperature is lowered, the moment decreases toward the spin-only value, as expected.<sup>23</sup> Compared to **4**, the increased moment for **3** could be due to a relaxed (more toward octahedral) coordination

(21) Complex **4** precipitates out from MeCN solution at 77 K.

(22) Martin, L. L.; Martin, R. L.; Murray, K. S.; Sargeson, A. M. *Inorg. Chem.* **1990**, *29*, 1387.

(23) Cotton, F. A.; Wilkinson, G. *Advanced Inorganic Chemistry*, 5th ed.; Wiley: New York, 1988; p 720.

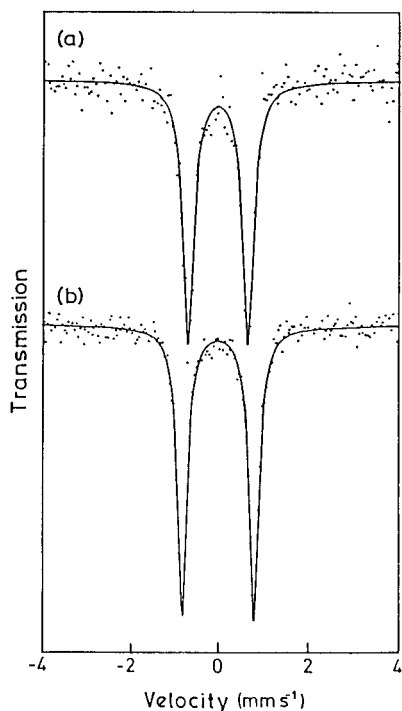


**Figure 3.** Mössbauer spectra of (a) Na[Fe(bpb)(CN)<sub>2</sub>] (**2**) and (b) [Fe(bpb)(CN)<sub>2</sub>] (**5**) at 300 K.

sphere.<sup>2</sup> For **4** in the solid state, the orbital contribution is much reduced, implying its distorted coordination sphere. However, in solution the geometry is more toward octahedral.

To substantiate the spin states, as well as to check the purity of the cyanide complexes **2** and **4**, Mössbauer spectral measurements at 300 K were performed, in the absence of an applied magnetic field. Each complex displays a symmetric doublet, which was analyzed as described previously.<sup>1</sup> The spectra of **2** and **4** are displayed in Figures 3 and S7 (Supporting Information), respectively. The  $\Delta E_Q$  values are consistent with the  $S = 1/2$  state.<sup>4a</sup>

**(b) Oxidized Complexes.** To obtain a better understanding of the electronic structure of the oxidized complexes, we have studied their temperature-dependent magnetic behavior (for **5**, 25–300 K; for **6**, 63–300 K). The  $\mu_{\text{eff}}$  values at 300 K reveal the quenching of the unpaired spins, in sharp contrast to those for **2** and **4** (Table 1). The  $\mu_{\text{eff}}$  values for **5** and **6** monotonically decrease with a lowering in temperature. The magnetic behavior of **5** (Figure 4) and **6** (Figure S8, Supporting Information) point toward the existence of strong antiferromagnetic coupling. Using eq 2, the best least-squares fit ( $g$  and TIP were fixed at 2.00 and  $120 \times 10^{-6} \text{ cm}^3 \text{ mol}^{-1}$ , respectively) obtained gave  $J \approx -520 \text{ cm}^{-1}$  and  $P = 3.11 \times 10^{-2}$  for **5** and  $J \approx -496 \text{ cm}^{-1}$  and  $P = 13.4 \times 10^{-2}$  for **6**. Given the presence of a considerable number of paramagnetic impurities (particularly in **6**), we are not in a position to distinguish between the  $J$  values of **5** and **6**. However, based on the data, we put a lower limit of  $\approx 450 \text{ cm}^{-1}$  on  $-2J$ .

Further evidence confirming the identity of **5** and **6** as  $\pi$ -radical cation complexes of low-spin iron(III) and not iron(IV)<sup>8b,24</sup> was obtained via Mössbauer spectral data (Table 1). The case of **5** is displayed in Figure 3. That the Mössbauer spectrum of **6** (Figure S9, Supporting Information) is almost identical to those of the parent compound **4** is compelling evidence that oxidation has occurred at the ligand in a site remote from the iron atom.

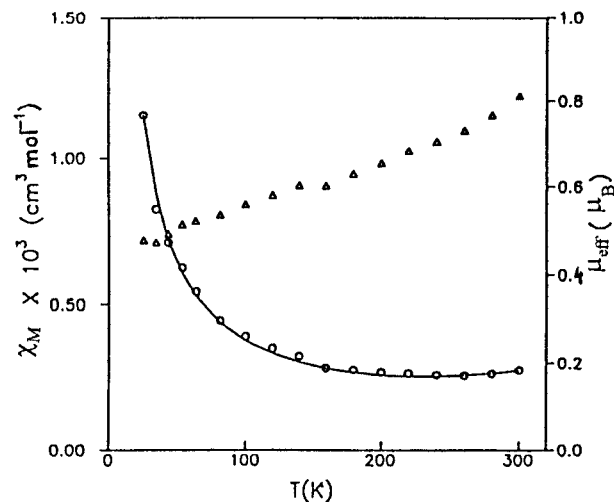


**Figure 4.** Temperature dependence (25–300 K) of the molar magnetic susceptibility (O) and magnetic moment ( $\Delta$ ) for [Fe(bpb)(CN)<sub>2</sub>] (**5**). The solid line represents theoretical fit using the equation described in the text.

**Nature of Oxidized Complexes.** A long-standing problem in the redox chemistry of metal complexes of ligands<sup>25–28</sup> (including porphyrins)<sup>27,28</sup> that are themselves potential sites of facile electron transfer is identifying whether the site of redox is metal-centered or ligand-centered. Since Mössbauer isomer shift ( $\delta$ ) values are generally quite sensitive to the oxidation state of the metal atom, the observation that the  $\delta$  values between **2** and **5** and between **4** and **6** are almost identical, suggests that the oxidation of **2** and **4** is essentially ligand-based rather than metal-centered. Moreover, the oxidation results in a pronounced increase (vide supra) in the C–O IR stretching frequencies of  $\nu(\text{amide I})$  vibration, suggestive of ligand oxidation.

In line with their magnetic behavior ( $S = 0$  state), complexes **5** and **6** are EPR silent (Table 1). In CDCl<sub>3</sub> solution (300 K), complex **6** displays a clean <sup>1</sup>H NMR spectrum (Figure 5), attesting to its diamagnetic ground state. The remarkably simple spectrum is due to its symmetric structure in solution (cf. solution state EPR spectrum of **4**). Assignment of the signals (Experimental Section) has been made through consideration of relative peak areas and comparison with free-ligand spectra.

If iron sites in **5** and **6** had expected  $C_{2v}$  symmetry, then the  $d_{xy}$  orbital would have  $a_2$  and the ligand  $\pi$  orbital  $a_1$  symmetry, and hence they would be orthogonal. Consequently, there would be no overlap between the metal orbital and the ligand orbital, and ferromagnetic coupling would be seen.<sup>27</sup> However, if we invoke nonplanar distortion of the present equatorial ligands, iron site symmetry would be lowered from  $C_{2v}$ . The effect is to remove the orthogonality between the metal  $d_{xy}$  orbital and the

- (25) (a) Pal, C. K.; Chattopadhyay, S.; Sinha, C.; Chakravorty, A. *Inorg. Chem.* **1994**, *33*, 6140 and references therein. (b) Shivakumar, M.; Pramanik, K.; Ghosh, P.; Chakravorty, A. *Inorg. Chem.* **1998**, *37*, 5968 and references therein. (c) Schwach, M.; Hausen, H.-D.; Kaim, W. *Inorg. Chem.* **1999**, *38*, 2242 and references therein.
- (26) (a) Warren, L. F. *Inorg. Chem.* **1977**, *16*, 2814. (b) Peng, S.-M.; Chen, C.-T.; Liaw, D.-S.; Chen, C.-I.; Wang, Y. *Inorg. Chim. Acta* **1985**, *101*, L31. (c) Peng, S.-M.; Liaw, D.-S. *Inorg. Chim. Acta* **1986**, *113*, L11.
- (27) (a) Scholz, W. F.; Reed, C. A.; Lee, Y. Ja; Scheidt, W. R.; Lang, G. *J. Am. Chem. Soc.* **1982**, *104*, 6791. (b) Gans, P.; Buisson, G.; Duée, E.; Marchon, J.-C.; Erler, B. S.; Scholz, W. F.; Reed, C. A. *J. Am. Chem. Soc.* **1986**, *108*, 8, 1223. (c) Scheidt, W. R.; Song, H.; Haller, K. J.; Safo, M. K.; Orosz, R. D.; Reed, C. A.; Debrunner, P. G.; Schulz, C. E. *Inorg. Chem.* **1992**, *31*, 939.
- (28) Buisson, G.; Deronzier, A.; Duée, E.; Gans, P.; Marchon, J.-C.; Regnard, J.-R. *J. Am. Chem. Soc.* **1982**, *104*, 6793.

(24) Cummins, C. C.; Schrock, R. R. *Inorg. Chem.* **1994**, *33*, 395.

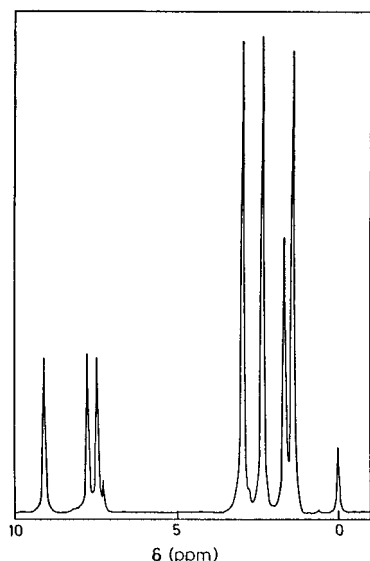


**Figure 5.**  $^1\text{H}$  NMR (400 MHz) spectrum of  $[\text{Fe}(\text{Me}_6\text{bpb})(\text{CN})_2]\cdot\text{H}_2\text{O}$  (**6**) in  $\text{CDCl}_3$  at 300 K.

1,2-diaminobenzene ring  $\pi$  orbital (both orbitals would have a symmetry in point group  $C_2$ ), providing a pathway for intramolecular  $d-\pi$  coupling (antiferromagnetic exchange) accounting for the observed diamagnetism. Thus, based on magnetic orbital symmetry expectations, we can say that in **5** and **6** the ligands are probably *not* planar.

### Summary and Conclusions

The data reported herein indicate that stable  $\pi$ -radical cation complexes of low-spin iron(III) of dianionic dipeptide ligands

can be isolated in analytically pure form for detailed characterization. To the best of our knowledge, this report documents the first example of such complexes with a tetradentate pyridine amide ligand system. The ligand framework provides nonmacrocyclic diamido *N*-coordination in the equatorial plane. The stabilization is achieved by an intramolecular antiferromagnetic coupling with a low-spin iron(III) center. The proposed electronic structure of these complexes ( $S = 0$  ground state) is substantiated by the observation of a  $^1\text{H}$  NMR spectrum in the  $\delta$  0–10 range.

**Acknowledgment.** This work is supported by grants from the Council of Scientific and Industrial Research and Department of Science and Technology, Government of India, New Delhi. We sincerely thank Dr. H. C. Verma of our Physics Department for his help with Mössbauer spectral measurements. Constructive comments of reviewers were very helpful at the revision stage.

**Supporting Information Available:** IR spectra of **2** and **5** (Figure S1), **4** and **6** (Figure S2); EPR spectrum of **4** in the polycrystalline state at 77 K (Figure S3); plots of reciprocal molar magnetic susceptibility vs temperature for **2–4** (Figures S4–S6); Mössbauer spectrum of **4** at 300 K (Figure S7); plot of molar magnetic susceptibility vs temperature for **6** (Figure S8), and Mössbauer spectrum of **6** at 300 K (Figure S9). This material is available free of charge via the Internet at <http://pubs.acs.org>.

IC9909734